https://jos.unsoed.ac.id/index.php/exj/index

E-ISSN : xxxxxxxxx
P-ISSN : xxxxxxxxx

EarthXplorer Journal

Vol 01 No 02 2026

RESEARCH ARTICLE

Understanding Riverbed Dynamics Through Grain-Size Analysis: Evidence from the headwater of Boyong River

Fathan Hanifi Mada Mahendra [1,*], Egy Erzagian[1], Ilham Pratama[1], Raja Susatio[2], Thema Arrisaldi[3]

[1] Geological Engineering Department, Universitas Jenderal Soedirman, Jl. Mayor Jenderal Sungkono Km. 5, Blater, Purbalingga, Central Java, Indonesia 53371

[2] Environmental Science, Faculty of Mathematics and Natural Sciences, Universitas Sebelas Maret, Jl. Ir. Sutami No.36, Surakarta, Central Java, Indonesia 57126

[3] Kyushu University, 744 Motooka, Nishi-ku, Fukuoka, 819-0395, Japan

* Corresponding author : fathan.hanifi@unsoed.ac.id
Tel.:+62-831-4482-0004

Received: Dec 15, 2025; Accepted: Jan 31, 2026.

Abstract

This study examines downstream variations in grain-size characteristics along the Boyong River, Yogyakarta, Indonesia, a volcaniclastic fluvial system with steep headwater gradients and sabo dams. The river was selected to evaluate the influence of channel slope reduction and anthropogenic sediment-control structures on sediment transport along a longitudinal profile. Three sediment samples (SBY1, SBY2, and SBY3) were collected from successive upstream-to-downstream reaches to capture spatial hydraulic changes.

Grain-size analysis was conducted using sieve data expressed in phi (ϕ) units and evaluated through two statistical approaches. Parameters analyzed include mean grain size, sorting, skewness, and kurtosis. Digital Elevation Model (DEM) analysis quantified slope differences among sites and related topographic gradients to sedimentological trends. Both analytical methods reveal a downstream fining trend. The upstream site (SBY1), located on the steepest slope, is dominated by coarser and sorted medium sand, indicating high flow capacity and competency. The middle reach (SBY2) contains finer and poorly sorted sediments, reflecting transport conditions as efficiency decreases. The downstream site (SBY3) exhibits the finest and poorly sorted material, consistent with reduced slope and diminished flow capacity. An increase in fine-grained fractions (>4 ϕ; silt and clay) downstream indicates enhanced suspended-load deposition. Minor discrepancies between methods occur mainly in skewness and kurtosis values, yet both approaches show consistent trends.

Overall, sediment transport along the Boyong River is governed by slope reduction and modified by sabo dams, which reduce flow velocity, disrupt sediment continuity, and promote sediment retention, enhancing downstream fining. These findings clarify fluvial responses to geomorphic and anthropogenic controls.

Keywords: Grain-size analysis; Boyong River; Downstream fining; Sabo dams impact; Fluvial sediment dynamics

1. Introduction

Sediment grain-size characteristics are fundamental indicators of riverbed dynamics because they reflect the interaction between sediment supply, transport processes, and river hydraulic conditions (Lepesqueur et al., 2019; Singh et al., 2007; Staudt et al., 2019; Zhang et al., 2025). Variations in grain-size parameters, such as mean size, sorting, skewness, and kurtosis record changes in flow capacity, depositional mechanisms, and spatial energy distribution along the river channel (Inman, 1952; McLaren and Bowles, 1985). Consequently, grain-size analysis is a widely adopted tool to interpret sediment transport behaviour, channel adjustment, and textural variations in fluvial systems, particularly in environments with abundant and rapidly renewed sediment supply, as documented by Church and Kellerhals, (1978); Okeyode and Jibiri, (2012); Rajganapathi et al., (2013); Surian, (2002); Wan Mohtar et al., (2017).

These concepts are also relevant in a volcanically influenced volcanic system where sediments are abundant and largely unconsolidated. The Boyong River represents a clear example of the system as it functions as one of the primary channels for sediment derived from Mount Merapi, one of the most active volcanoes in Indonesia. During periods of rainfall, unconsolidated pyroclastic and volcaniclastic materials stored on the upper slopes of Merapi are readily remobilized and transported downstream through the Boyong River system (Kurniawan et al., 2020; Lavigne et al., 2000) carrying the volume of over 2.5 million m^3 sediment materials in 1994 (Abdurachman et al., 2000). This process results in episodic yet continuous sediment transportation, creating highly dynamic riverbed conditions that are strongly controlled by variations in river flow capacity rather than long-term equilibrium.

This study aims to analyze and compare riverbed grain-size characteristics at three sampling locations along the upstream reach of the Boyong River. Although all sampling sites are located within the headwater zone, differences in distance from sediment sources and rainfall-driven transport intensity are expected to influence grain-size distributions and depositional patterns. By examining spatial variations in grain-size parameters, this research also tries to determine how flow capacity governs sediment transport efficiency and riverbed adjustment in volcanically influenced fluvial systems.

Overall, this study provides insight into the linkage between sediment granulometry and river dynamics in an active volcanic setting. The results are expected to contribute to fluvial sedimentology studies and support river management and hazard mitigation efforts in Merapi's downstream areas, where sediment transport processes pose both environmental and societal challenges.

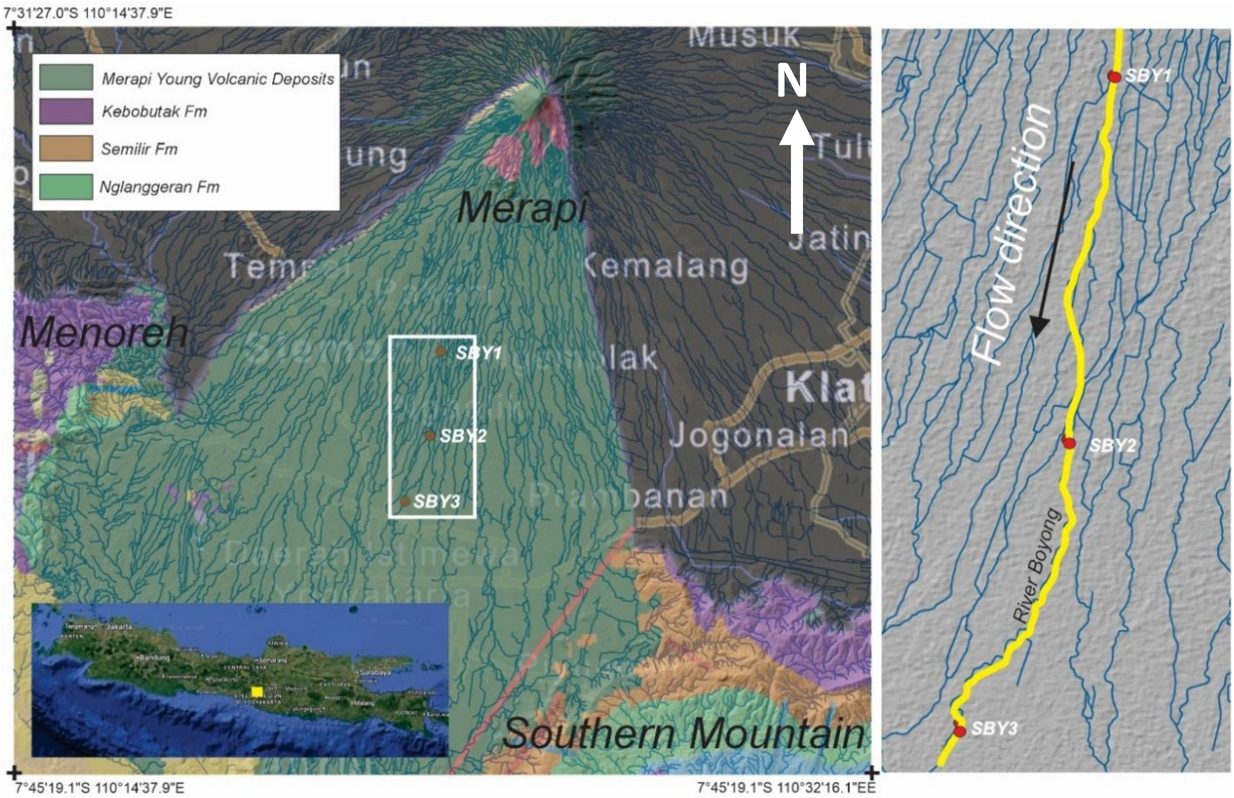

Figure 1. Location and geology of the study area

2. Study area

The Boyong River (Figure 1) is located on the southern flank of Mount Merapi, Yogyakarta, Indonesia, and serves as a primary natural drainage systems transporting volcaniclastic material from the summit area toward the southern lowlands (Brontowiyono et al., 2011; Hadmoko, 2024). As shown in the geological map (Rahardjo et al., 1977), the study area lies within the distribution of Merapi Young Volcanic Deposits, which dominate the upper catchment and extend along the Boyong River. These deposits represent products of recent volcanic activity and are characterized by high lithological variability and loose clastic materials (Lavigne, 2004).

In addition to transporting unconsolidated volcanic material, the Boyong River actively erodes the underlying Merapi Young Volcanic units. These units are generally composed of tuff, volcanic ash, breccia, agglomerate, and lava flow deposits. Fluvial incision and lateral erosion along the river channel continuously rework these lithologies, contributing fresh volcaniclastic fragments to the river system. As a result, riverbed sediments reflect a combination of primary volcanic deposition and secondary fluvial reprocessing, producing complex grain-size distributions.

Topographically, the study area exhibits a steep radial drainage pattern typical of volcanic edifices, with river channels oriented downslope from

Mount Merapi. A rapid decrease in elevation from north to south generates a high longitudinal gradient that enhances river flow capacity during periods of high discharge. This strong gradient promotes efficient sediment transport and frequent reworking of channel deposits, especially during rainfall-induced flood and lahar events.

Human intervention also plays a role in modifying sediment dynamics within the Boyong River system. A series of sabo dams have been constructed along the river to reduce flow energy and trap coarse volcaniclastic material (Destania and Syarifudin, 2021; Hidayat et al., 2021). These structures are designed to mitigate volcanic debris-flow hazards but may locally alter sediment transport processes(Kim et al., 2017). Reduced flow energy upstream and downstream of sabo dams can promote finer-grained deposition compared to natural conditions, potentially influencing the spatial distribution of grain-size characteristics along the study reach.

Three sampling locations (SBY1, SBY2, and SBY3) were selected along the upstream segment of the Boyong River, following the main channel from north to south. Although all sites are located within the same volcanic depositional unit, variations in distance from sediment sources, local slope, erosional exposure of volcanic lithologies, and the presence of sabo dams are expected to influence grain-size distributions and riverbed texture. This integrated geological, topographic, and anthropogenic setting provides a robust framework for interpreting grain-size variability and riverbed dynamics in a volcanically active fluvial system.

3. Methods

Sediment samples were collected from three locations along the upstream reach of the Boyong River, referred to as SBY1, SBY2, and SBY3. All sampling sites are located within the headwater zone of the river and lie along the main channel, following the general flow direction from north to south. The selection of these sites was designed to capture spatial variations in riverbed sediment characteristics while minimizing differences related to downstream geomorphic transitions.

At each location, riverbed sediment was sampled from active channel deposits to represent recent sediment transport and depositional processes. Grain-size analysis was conducted to characterize the sediment distribution and infer transport and depositional conditions. The collected samples were first oven-dried to remove moisture content and ensure consistent dry-weight measurements. Drying was performed until a constant weight was achieved, minimizing the influence of water content on grain-size proportions.

After drying, the samples were homogenized and reduced using the quartering technique to obtain a representative subsample of 100 g following (Harvey Blatt, 1985). This procedure was applied to minimize sampling bias and ensure that the analyzed material adequately represented the original sediment population.The subsamples were then subjected to dry sieve analysis using a set of standard sieves corresponding to Wentworth phi (ϕ) intervals. The sieve sizes represent the following grain-size classes: 0–1ϕ, 1–2ϕ, 2–3ϕ, 3–4ϕ, and >4 ϕ. Each subsample was mechanically sieved to separate sediment fractions based on grain size. Following sieving, the sediment retained on each mesh was weighed, and the mass of each fraction was recorded. The weight data were then converted into percentage distributions to describe the grain-size composition of each sample.

Grain-size data were analyzed using both mathematical and graphical (Folk and Ward, 1957; Friedman, 1979; Lewis and McConchie, 1994) methods to ensure robust interpretation and cross-validation of results. Mathematical analysis was applied to calculate statistical grain-size parameters, including mean grain size, sorting, skewness, and kurtosis. Graphical analysis was performed using cumulative grain-size curves to derive equivalent parameters and to assess sediment distribution patterns visually.

The use of both analytical approaches allows for validation of grain-size characteristics and reduces uncertainty associated with relying on a single method.

Topographic Data Analysis

In addition to sedimentological analysis, Digital Elevation Model (DEM) data were utilized to examine the topographic characteristics of the study area. Contour and slope analyses derived from the DEM were used as supporting data to interpret spatial variations in sediment distribution and river flow behaviour. This topographic information provides context for understanding the influence of longitudinal gradient and local relief on sediment transport and deposition along the upstream Boyong River.

4. Data

Grain-size analysis of riverbed sediments from the Boyong River was conducted using both mathematical and graphical approaches in order to obtain a comprehensive and validated description of sediment characteristics. The results from both methods are presented to evaluate grain-size distribution parameters and to assess their consistency. The analyzed parameters include mode, mean grain size, sorting (variance), skewness, and kurtosis. These statistical measures describe the central tendency, dispersion, and shape of the grain-size distribution, which are essential for interpreting sediment transport and depositional processes in fluvial environments.

4.1. Mathematical method

Mathematical analysis was applied to calculate grain-size statistics directly from the weight-percentage data obtained from sieve analysis. All calculations were performed using grain-size classes expressed in phi (∅) units based on the Wentworth scale. The mathematical approach allows quantitative comparison between samples and provides objective statistical measures. The grain-size parameters were calculated using the following equations (1)-(4):

Mean

$$x\emptyset = \frac{\sum fm}{N} \qquad (1)$$

Variance (standard deviation)

$$\sigma\emptyset = \sqrt{\frac{\sum f(m-X\emptyset)^2}{100}} \qquad (2)$$

Skewness

$$Sk\emptyset = \frac{\sum f(m-X\emptyset)^3}{100\sigma\emptyset^3} \qquad (3)$$

Kurtosis

$$K\emptyset = \frac{\sum f(m-X\emptyset)^4}{100\sigma\emptyset^4} \qquad (4)$$

Result using mathematical method are presented in Table 1. The sediment sample from SBY1 (Table 1A) shows a mean grain size of M = 1.26 ϕ, with a dominant mode at 1.2 ϕ (medium sand). Sorting values have variance of 0.97, suggesting moderately sorted sediment conditions. Skewness is 1.11 (*very fine skewed*), indicating a tendency toward coarse/fine skewness, while kurtosis values (K =3.49) suggest an extremely leptokurtic grain-size distribution. These characteristics reflect relatively higher flow capacity and active sediment reworking in the upstream area.

Table 1. Grain-size analyses using mathematic method

A

Interval	Mid Value (m)	Weight Freq. (%)	fm	Deviation(m-x)	$(m-x)^2$	$f(m-x)^2$	$(m-x)^3$	$f(m-x)^3$	$(m-x)^4$	$f(m-x)^4$
0-1	0.50	54.08	27.04	-0.76	0.57	30.87	-0.43	-23.33	0.33	17.62
1-2	1.50	22.74	34.12	0.24	0.06	1.36	0.01	0.33	0.00	0.08
2-3	2.50	18.03	45.08	1.24	1.55	27.93	1.93	34.75	2.40	43.25
3-4	3.50	3.82	13.37	2.24	5.04	19.25	11.31	43.20	25.38	96.96
>4	4.50	1.32	5.94	3.24	10.53	13.90	34.15	45.09	110.81	146.29
Total		100.00	125.56	6.22	17.74	93.30	46.97	100.05	138.91	304.21
Mean (x)	**1.26**	**Variance σ**		**0.97**	**Skewness SK**		**1.11**	**Kurtosis K**		**3.49**

B

Interval	Mid Value (m)	Weight Freq. (%)	fm	Deviation(m-x)	$(m-x)^2$	$f(m-x)^2$	$(m-x)^3$	$f(m-x)^3$	$(m-x)^4$	$f(m-x)^4$
0-1	0.50	49.12	24.56	-0.82	0.68	33.34	-0.56	-27.47	0.46	22.63
1-2	1.50	29.49	44.23	0.18	0.03	0.91	0.01	0.16	0.00	0.03
2-3	2.50	14.73	36.83	1.18	1.38	20.38	1.63	23.97	1.91	28.19
3-4	3.50	3.22	11.26	2.18	4.74	15.23	10.30	33.14	22.42	72.12
>4	4.50	3.45	15.51	3.18	10.09	34.77	32.04	110.44	101.76	350.78
Total		100.00	132.39	5.88	16.92	104.64	43.42	140.24	126.56	473.75
Mean (x)	**1.32**	**Variance σ**		**1.02**	**Skewness SK**		**1.31**	**Kurtosis K**		**4.33**

C

Interval	Mid Value (m)	Weight Freq. (%)	fm	Deviation(m-x)	$(m-x)^2$	$f(m-x)^2$	$(m-x)^3$	$f(m-x)^3$	$(m-x)^4$	$f(m-x)^4$
0-1	0.50	46.25	23.13	-1.01	1.01	46.92	-1.02	-47.26	1.03	47.60
1-2	1.50	19.23	28.85	-0.01	0.00	0.00	0.00	0.00	0.00	0.00
2-3	2.50	25.18	62.94	0.99	0.99	24.82	0.98	24.64	0.97	24.46
3-4	3.50	6.21	21.75	1.99	3.97	24.68	7.91	49.18	15.77	98.00
>4	4.50	3.12	14.05	2.99	8.96	27.96	26.81	83.69	80.22	250.48
Total		100.00	150.72	4.96	14.93	124.38	34.68	110.25	98.00	420.54
Mean (x)	**1.51**	**Variance σ**		**1.12**	**Skewness SK**		**0.79**	**Kurtosis K**		**2.72**

Sample SBY2 (Table 1B) is characterized by a mean grain size of M= 1.32 ϕ, which is finer than SBY1. The mode occurs at 1.08 ϕ, and sorting values (variance = 1.02) indicate poorer sorting compared to the upstream site. Skewness values (Sk = 1.31) suggest a very fine-skewed curve, while kurtosis (K = 4.33) indicates an extremely leptokurtic distribution. This pattern reflects transitional hydraulic conditions and poorer sediment sorting during downstream transport compared to SBY1.

The SBY3 (Table 1C) sample exhibits the finest grain size among the three locations, with a mean of M = 1.51 ϕ finer compared to medium sand size in SBY1 and SBY2. Mode is at 0.9 ϕ. Sorting values (variance = 1.12) indicate poorly sorted sediments, while skewness (Sk = 0.79) shows a clear tendency toward fine skewness. Kurtosis (K = 2.72) suggests a very leptokurtic distribution, reflecting lower flow capacity and enhanced

fine-grained deposition, possibly influenced by reduced channel gradient and the presence of sabo dams.

4.2. *Graphical method*

The graphical statistical method was applied to determine grain-size distribution parameters based on percentiles obtained from cumulative grain-size curves. Cumulative curves were constructed using sieve analysis results expressed in phi (ϕ) units following the Wentworth scale. This method allows statistical parameters to be derived directly from the shape of the distribution and is widely used in sedimentological studies. From the cumulative curves, specific percentile values were read and used to calculate key grain-size statistics, including mean grain size, sorting, skewness, and kurtosis as seen in formulas (5)-(8).

Mean

$$M = \frac{\emptyset 16+\emptyset 50+\emptyset 84}{3} \quad (5)$$

Sorting

$$\sigma = \frac{\emptyset 84+\emptyset 16}{4} + z\frac{\emptyset 95-\emptyset 5}{6.6} \quad (6)$$

Skewness

$$SK = \frac{\emptyset 84+\emptyset 16-2\emptyset 50}{2(\emptyset 84-\emptyset 16)} + \frac{\emptyset 95+\emptyset 5+2\emptyset 50}{2(\emptyset 95-\emptyset 5)} \quad (7)$$

Kurtosis

$$K = \frac{\emptyset 95-\emptyset 5}{2.44(\emptyset 75-\emptyset 25)} \quad (8)$$

The result of the graphical method is presented in Table 2. A general overview using a graphical method exhibits a mean value range of 1.23-1.50 ϕ, or predominantly composed of medium sand (Figure 2). The finest medium sand was found in SBY3, portraying a probability of decreasing transport energy to the downstream.

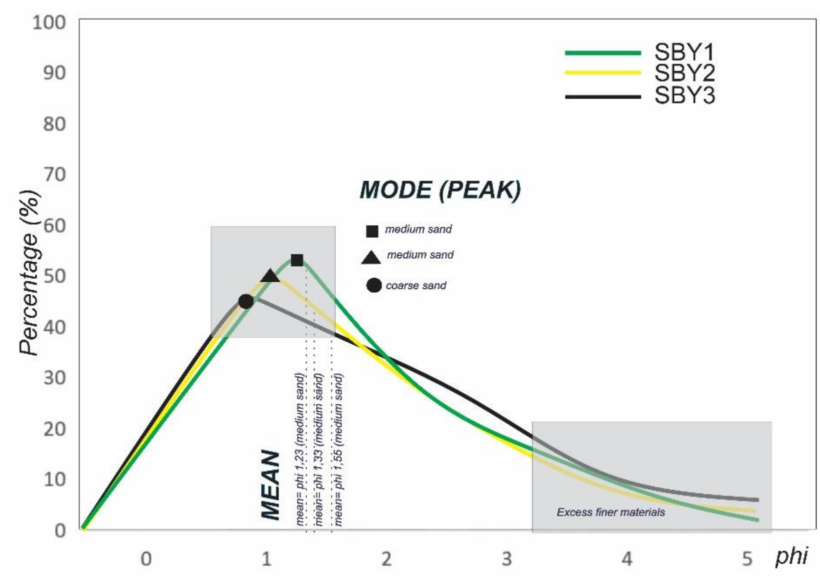

Figure 2. Mean and mode curves for research location

Unlike the results from the mathematical methods, the sortation using graphical methods shows significantly different decreasing values downstream, respectively 1.24, 1.20, and 1.07, classified as poorly sorted sediments (Figure 3). The skewness trendline also has a different decreasing pattern compared to the mathematical method respectively 0.52, 0.41, and 0.24 classified as very fine skewed to fine skewed. The Kurtosis shows relatively lower value compared to the mathematical method for SBY1, SBY2, and SBY3 respectively 1.08, 1.21, and 0.69 from mesokurtic to platykurtic.

Table 2. Grain-size analyses using graphical method

Sample	Φ5	Φ16	Φ25	Φ50	Φ75	Φ84	Φ95
SBY1	0.1	0.2	0.4	0.9	2	2.6	4.3
SBY2	0.1	0.3	0.5	1.1	1.9	2.6	4.25
SBY3	0.1	0.4	0.57	1.3	2.4	2.8	3.2

Mean	*Sortation*	*Skewness*	*Kurtosis*
1.23	1.24	0.52	1.08
1.33	1.20	0.41	1.21
1.50	1.07	0.24	0.69

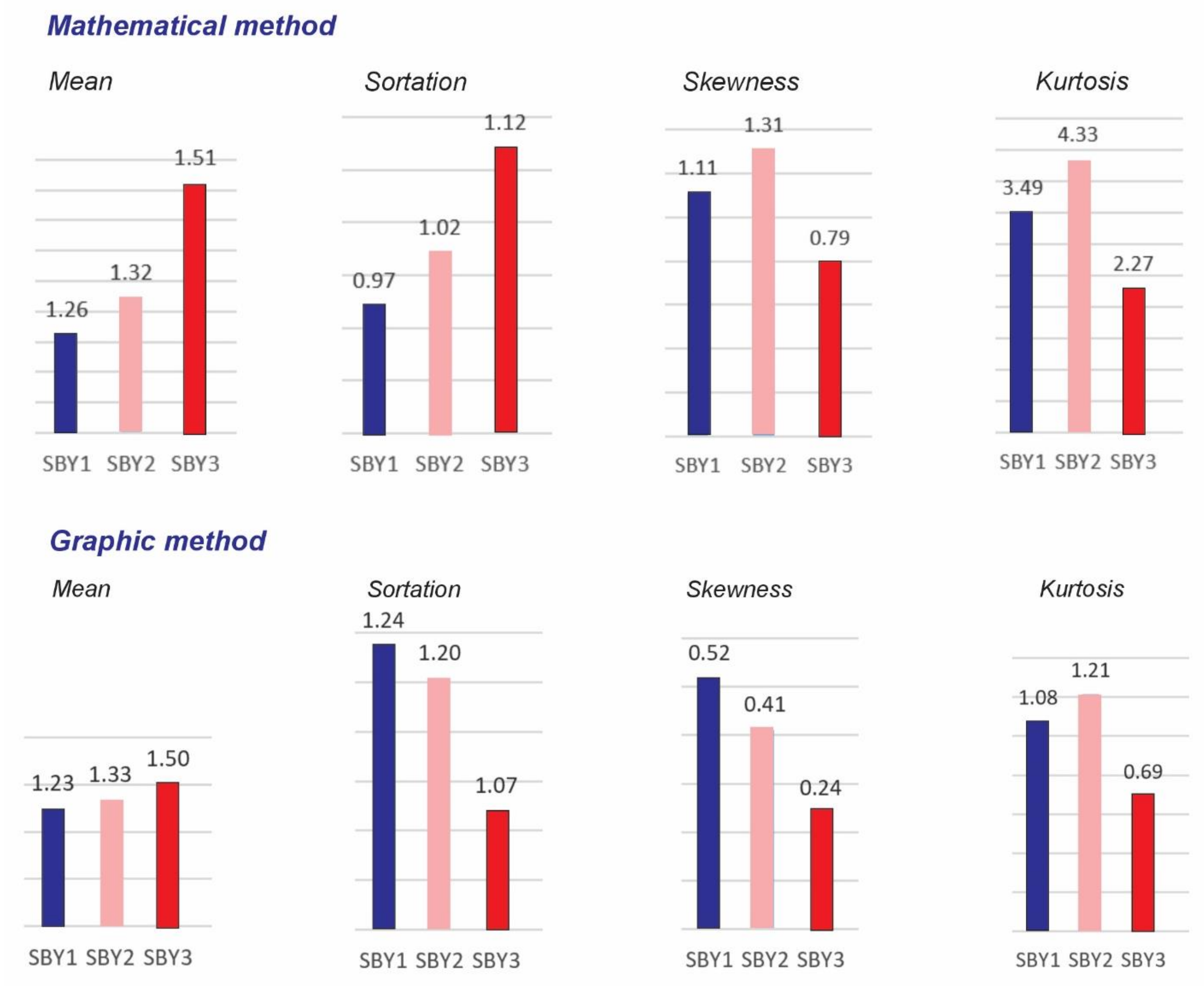

Figure 3. Comparison of grain-size statistical analyses (a) mathematical method, (b) graphical method

5. Discussion

The upstream condition can be seen in Figure 5A & 5C classified as a cascade channel type with the characteristic of Boulders-cobble with several coarser bedload (Montgomery and Buffington, 1997). Although the upstream reach is predominantly characterized by coarse gravel deposits, grain-size analysis was focused on the sand fraction because it provides a more sensitive and statistically robust record of fluvial hydraulic processes (Griffiths et al., 1962; Ingersoll, 1990; Ingersoll et al., 1993). Gravel transport in headwater channels is largely controlled by threshold conditions and sediment supply, resulting in discontinuous and locally variable size distributions. In contrast, sand-sized particles are continuously mobilized and hydraulically sorted under a wider range of flow conditions, making them more responsive to subtle variations in flow capacity and competency. Consequently, analysis of the sand fraction allows for consistent downstream comparison and more reliable interpretation of longitudinal changes in fluvial energy, even within gravel-bed river systems.

Grain-size data derived from both mathematical and graphical methods show a clear downstream fining trend from SBY1 to SBY3 (Figure 3), reflecting a progressive reduction in flow capacity (the ability of the flow to transport sediment) and flow competency (the maximum grain size the flow can mobilize). Although all samples fall within the medium-sand range, the systematic variations in mean size, sorting, skewness, and kurtosis correspond strongly to spatial changes in hydraulic and geomorphic conditions.

DEM analysis indicates a 3–5° decrease in channel slope between the sampling sites, with SBY1 located on the steepest gradient. A higher slope results in greater flow capacity and competency, allowing the transport of coarser material and more efficient hydraulic reworking. This is reflected in SBY1, which exhibits the coarsest mean grain size (1.26ϕ), relatively better sorting, strong leptokurtosis, and very fine skewness—characteristics typical of high-competency upstream flows.

At SBY2, the slight reduction in slope is accompanied by a measurable decline in flow competency, producing a slightly finer mean grain size (1.32 ϕ) and poorer sorting. The increase in skewness and high kurtosis values suggests selective transport, where finer particles begin to accumulate while coarser grains are transported less effectively. This indicates transitional hydraulic conditions between the high-energy upstream segment and lower-energy downstream areas.

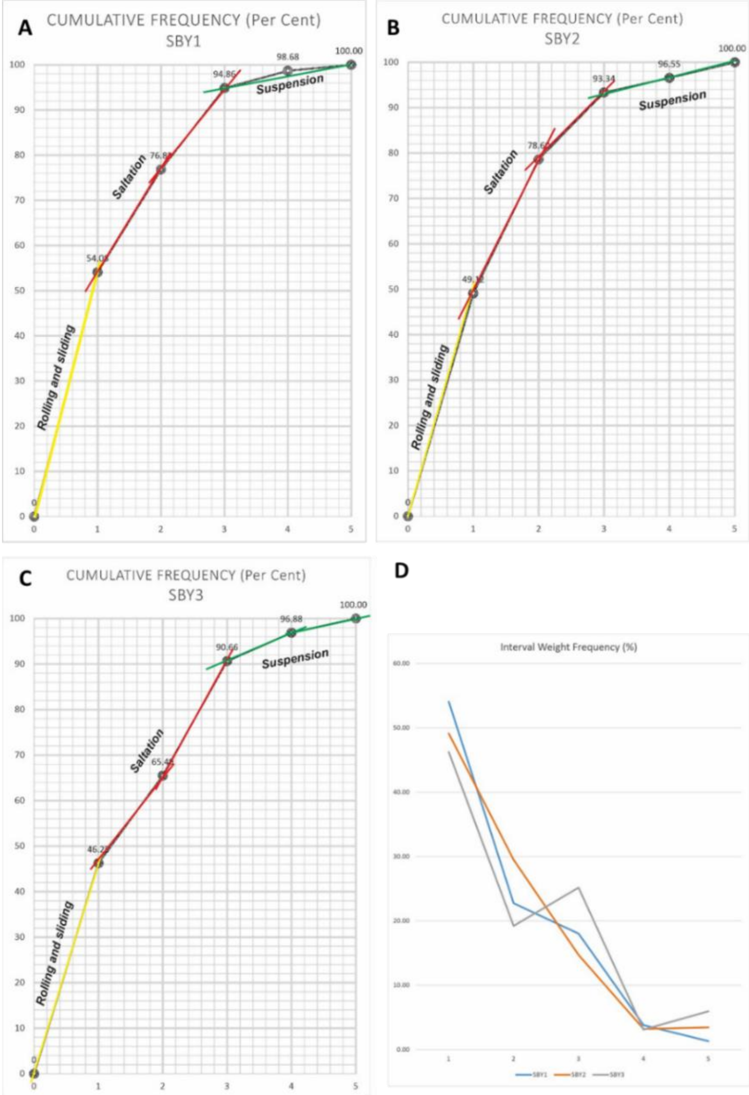

Figure 4. Comparison of grain-size cumulative frequencies in % A. SBY1 ; B. SBY2; C. SBY3, D. Interval weight frequency showing predominant coarse-medium sand compared to other finer sediments (silt and clay)

The most pronounced changes appear at SBY3. Its lower gradient corresponds with the lowest flow capacity and competency, resulting in the finest mean grain size (1.51 ϕ), the poorest sorting, and reduced kurtosis. However, slope reduction alone does not fully explain the high proportion of fine-grained material. The presence of sabo dams introduces significant additional hydraulic controls (Figure 5B). These structures reduce flow velocity, disrupt sediment continuity, and promote the deposition of finer suspended-load particles.

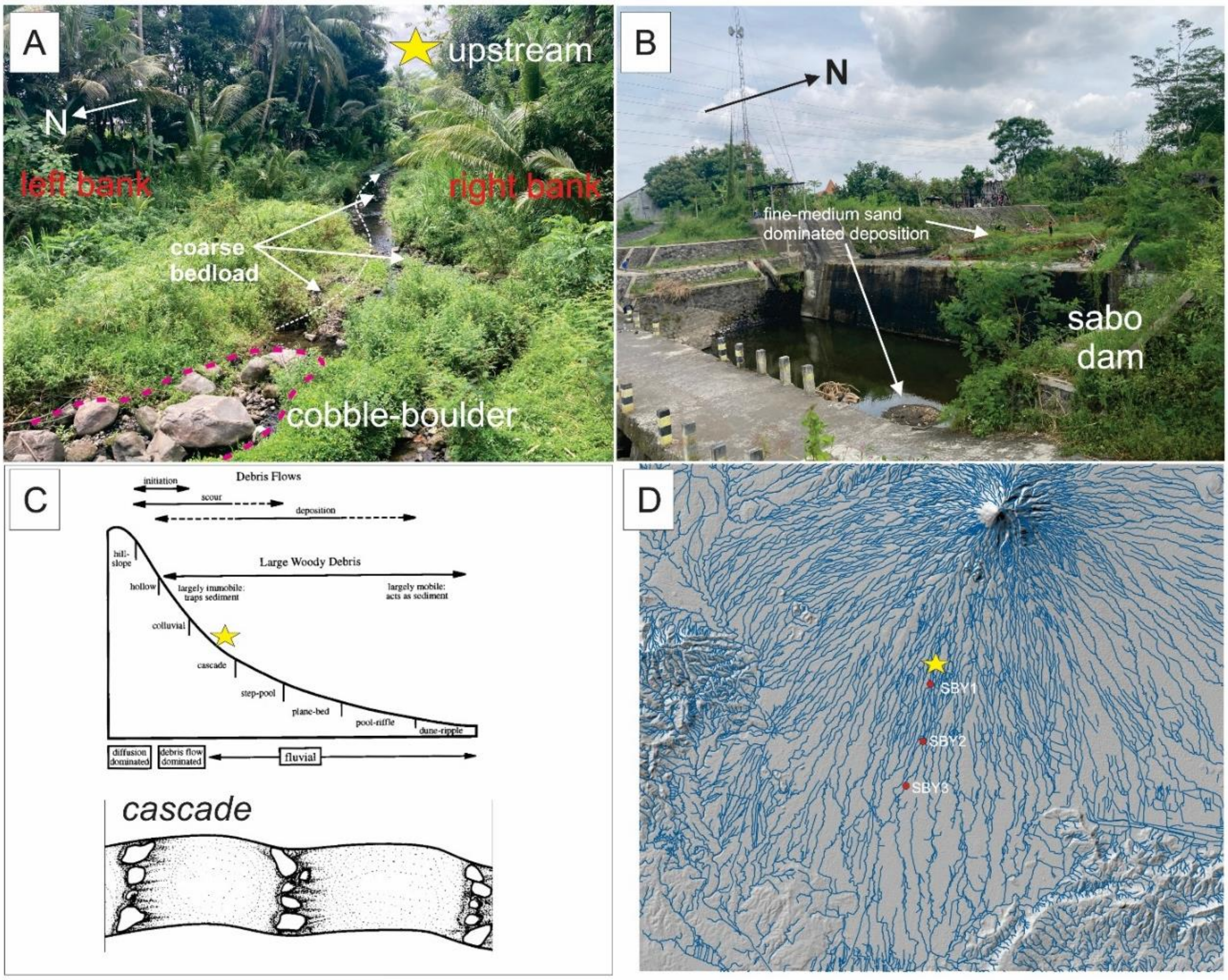

Figure 5. Field photography A) Upstream condition showing a dominant boulder and coarse sediment bedload, B) Sabo dam between SBY1 and SBY2 showing significant fining change on sediment deposition, C) & D) Diagram modified from Montgomery and Buffington, (1997) showing the upstream location and cascade type of channel type

This effect is clearly supported by the increase in fine sediment fractions (>4 ϕ; silt and clay) downstream (Figure 5D). The proportion of fines is lowest in SBY1, increases in SBY2, and becomes highest in SBY3, demonstrating that sabo dams further reduce flow competency beyond what would be expected from slope decline alone. Their presence encourages early deposition of fine particles that would otherwise remain in suspension and be transported farther downstream. Although mathematical and graphical methods differ in magnitude particularly in skewness and kurtosis due to methodological sensitivity they consistently show the same downstream trends: fining grain size, decreasing sorting, and increasing fine material. The graphical method produces more moderate values, but the pattern remains consistent across both analytical approaches.

Overall, the integration of grain-size statistics, DEM-derived slope variations, and geomorphic controls indicates that sediment evolution along the Boyong River is governed by three main factors:

1. **Decreasing channel slope**, reducing flow capacity and competency;
2. **Natural downstream decline in hydraulic energy**, producing finer and more poorly sorted deposits; and
3. **Anthropogenic modification through sabo dams**, significantly enhancing the deposition of fine-grained sediment and altering natural sediment transport pathways.

This combined evidence highlights a transition from a high-capacity, high-competency upstream system to a low-capacity, fine-dominated depositional environment downstream.

The cumulative frequency curves for SBY1, SBY2, and SBY3 consistently show that most particles are transported predominantly through rolling–sliding and saltation processes. This is indicated by the steep rise in cumulative frequency within the coarser grain-size fractions (approximately 45–80%), where the transport energy is sufficient to mobilize sediment along the bed but not high enough to sustain full suspension. Only a very small proportion of the material enters the suspension load, as reflected by the subtle curvature and minimal increment in cumulative frequency near the finer fraction (above ~90%). This pattern demonstrates that the river's transport capacity is mainly bedload-dominated, with limited suspended load, which is characteristic of high-gradient headwater channels where coarse grains are repeatedly mobilized by traction and saltation while fine sediments remain scarce or only briefly entrained. The similarity of these trends across the three sampling points further suggests that the hydraulic conditions along this upstream segment remain consistently dominated by near-bed transport mechanisms rather than suspension-driven processes.

Conclusions

Grain-size analyses from both mathematical and graphical approaches reveal a consistent downstream fining trend along the Boyong River, driven by declining flow capacity and competency as channel slope decreases. The upstream site (SBY1), situated on the steepest gradient, contains coarser and better-sorted sediments, reflecting high-competency flows capable of mobilizing large grains through traction-dominated mechanisms. Progressing downstream to SBY2 and SBY3, the reduction in slope corresponds with finer mean grain sizes, poorer sorting, and lower kurtosis, indicating diminished hydraulic efficiency and reduced sediment-transport capability.

Interpretations from the cumulative frequency curves further support this trend: the majority of sediment at all three sites is transported through rolling–sliding and saltation (Figure 5A-C), with only a very small fraction entering suspension. This dominance of bedload transport highlights the energetic but near-bed–focused nature of sediment movement in this headwater system, where coarse materials are repeatedly reworked while true suspended-load transport remains limited.

The marked increase in fine-grained material (>4 ϕ) at SBY3 reflects not only natural downstream energy loss but also significant anthropogenic influence. Sabo dams disrupt sediment continuity by trapping fine suspended material upstream, thereby enhancing the downstream accumulation of finer fractions beyond what would result from slope changes alone.

Overall, the integrated sedimentological and geomorphic evidence characterizes the Boyong River as a system transitioning from a high-energy, coarse-dominated upstream environment to a lower-energy, fine-dominated depositional setting downstream—its evolution shaped jointly by natural gradient variation and engineered sediment-control structures.

Acknowledgements

The author gratefully acknowledges the Sedimentology Laboratory of Universitas Gadjah Mada for providing laboratory facilities and technical support for grain-size analysis. Sincere appreciation is extended to academic supervisors and lecturers for their valuable guidance, constructive feedback, and insightful discussions throughout the course of this research. The author also thanks colleagues and field partners for their assistance during fieldwork along the Boyong River, particularly in sediment sampling and data collection. Finally, gratitude is expressed to all individuals who contributed directly or indirectly to the completion of this study.

References

Abdurachman, E.K., Bourdier, J.-L., Voight, B., 2000. Nuées ardentes of 22 November 1994 at Merapi volcano, Java, Indonesia. J. Volcanol. Geotherm. Res. 100, 345–361. https://doi.org/10.1016/S0377-0273(00)00144-X

Brontowiyono, W., L., R., Hamidin, H., 2011. KEMAMPUAN TAMPUNGAN SUNGAI CODE TERHADAP MATERIAL LAHAR DINGIN PASCAERUPSI GUNUNGAPI MERAPI TAHUN 2010. J. Sains Teknol. Lingkung. 3, 81–87. https://doi.org/10.20885/jstl.vol3.iss2.art1

Church, M., Kellerhals, R., 1978. On the statistics of grain size variation along a gravel river. Can. J. Earth Sci. 15, 1151–1160. https://doi.org/10.1139/e78-121

Destania, H.R., Syarifudin, A., 2021. RADAR-BASED RAINFALL ESTIMATION IN BOYONG RIVER (BO-D5). Indones. J. Eng. Sci. 3, 007–019. https://doi.org/10.51630/ijes.v3i1.31

Folk, R.L., Ward, W.C., 1957. Brazos River bar [Texas]; a study in the significance of grain size parameters. J. Sediment. Res. 27, 3–26. https://doi.org/10.1306/74D70646-2B21-11D7-8648000102C1865D

Friedman, G.M., 1979. Differences in size distributions of populations of particles among sands of various origins: addendum to IAS Presidential Address. Sedimentology 26, 859–862. https://doi.org/10.1111/j.1365-3091.1979.tb00979.x

Griffiths, D.H., King, R.F., Rees, A.I., 1962. THE RELEVANCE OF MAGNETIC MEASUREMENTS ON SOME FINE GRAINED SILTS TO THE STUDY OF THEIR DEPOSITIONAL PROCESS. Sedimentology 1, 134–144. https://doi.org/10.1111/j.1365-3091.1962.tb00030.x

Hadmoko, D.S., 2024. Banjir Lahar Pembentukan Proses Dampak dan Mitigasinya. UGM PRESS.

Harvey Blatt, 1985. Provenance Studies and Mudrocks. SEPM J. Sediment. Res. Vol. 55. https://doi.org/10.1306/212F8611-2B24-11D7-8648000102C1865D

Hidayat, M., Legono, D., Wignyosukarto, B., Jayadi, R., Rahardjo, A.P., Hairani, A., Harsanto, P., Ikhsan, J., 2021. Flow Behavior of Boyong River as Revealed by Long-term Hydro-monitoring System. IOP Conf. Ser. Earth Environ. Sci. 930, 012023. https://doi.org/10.1088/1755-1315/930/1/012023

Ingersoll, R.V., 1990. Actualistic sandstone petrofacies: Discriminating modern and ancient source rocks. Geology 18, 733. https://doi.org/10.1130/0091-7613(1990)018%253C0733:ASPDMA%253E2.3.CO;2

Ingersoll, R.V., Kretchmer, A.G., Valles, P.K., 1993. The effect of sampling scale on actualistic sandstone petrofacies. Sedimentology 40, 937–953. https://doi.org/10.1111/j.1365-3091.1993.tb01370.x

Inman, D., 1952. Measures for Describing the Size Distribution of Sediments. SEPM J. Sediment. Res. Vol. 22. https://doi.org/10.1306/D42694DB-2B26-11D7-8648000102C1865D

Kim, Y., Nakagawa, H., Kawaike, K., Zhang, H., 2017. Study on hydraulic characteristics of sabo dam with a flap structure for debris flow. Int. J. Sediment Res. 32, 452–464. https://doi.org/10.1016/j.ijsrc.2017.05.001

Kurniawan, V.O., Mei, E.Y.W., Hadmoko, D.S., 2020. Pemodelan aliran lahar Gunung Api Merapi untuk perhitungan risiko kerugian pada penggunaan lahan terdampak di bantaran Sungai Boyong, Pakem, Sleman, D.I. Yogyakarta. J. Geogr. Lingkung. Trop. 3. https://doi.org/10.7454/jglitrop.v3i2.64

Lavigne, F., 2004. Rate of sediment yield following small-scale volcanic eruptions: a quantitative assessment at the Merapi and Semeru stratovolcanoes, Java, Indonesia. Earth Surf. Process. Landf. 29, 1045–1058. https://doi.org/10.1002/esp.1092

Lavigne, F., Thouret, J.-C., Voight, B., Young, K., LaHusen, R., Marso, J., Suwa, H., Sumaryono, A., Sayudi, D.S., Dejean, M., 2000. Instrumental lahar monitoring at Merapi Volcano, Central Java, Indonesia. J. Volcanol. Geotherm. Res. 100, 457–478. https://doi.org/10.1016/S0377-0273(00)00151-7

Lepesqueur, J., Hostache, R., Martínez-Carreras, N., Montargès-Pelletier, E., Hissler, C., 2019. Sediment transport modelling in riverine environments: on the importance of grain-size distribution, sediment density, and suspended sediment concentrations at the upstream boundary. Hydrol. Earth Syst. Sci. 23, 3901–3915. https://doi.org/10.5194/hess-23-3901-2019

Lewis, D.W., McConchie, D., 1994. Analytical Sedimentology. Springer US, Boston, MA. https://doi.org/10.1007/978-1-4615-2636-0

McLaren, P., Bowles, D., 1985. The Effects of Sediment Transport on Grain-Size Distributions. SEPM J. Sediment. Res. Vol. 55. https://doi.org/10.1306/212F86FC-2B24-11D7-8648000102C1865D

Montgomery, D.R., Buffington, J.M., 1997. Channel-reach morphology in mountain drainage basins. Geol. Soc. Am. Bull. 109, 596–611. https://doi.org/10.1130/0016-7606(1997)109%253C0596:CRMIMD%253E2.3.CO;2

Okeyode, I.C., Jibiri, N.N., 2012. Grain Size Analysis of the Sediments from Ogun River, South Western Nigeria. Earth Sci. Res. 2, p43. https://doi.org/10.5539/esr.v2n1p43

Rahardjo, W., Sukandarumidi, Rosidi, H., 1977. Peta Geologi Lembar Yogyakarta.

Rajganapathi, V.C., Jitheshkumar, N., Sundararajan, M., Bhat, K.H., Velusamy, S., 2013. Grain size analysis and characterization of sedimentary environment along Thiruchendur coast, Tamilnadu, India. Arab. J. Geosci. 6, 4717–4728. https://doi.org/10.1007/s12517-012-0709-0

Singh, M., Singh, I.B., Müller, G., 2007. Sediment characteristics and transportation dynamics of the Ganga River. Geomorphology 86, 144–175. https://doi.org/10.1016/j.geomorph.2006.08.011

Staudt, F., Mullarney, J.C., Pilditch, C.A., Huhn, K., 2019. Effects of grain-size distribution and shape on sediment bed stability, near-bed flow and bed microstructure. Earth Surf. Process. Landf. 44, 1100–1116. https://doi.org/10.1002/esp.4559

Surian, N., 2002. Downstream variation in grain size along an Alpine river: analysis of controls and processes. Geomorphology 43, 137–149. https://doi.org/10.1016/S0169-555X(01)00127-1

Wan Mohtar, W.H.M., Bassa, S.A., Porhemmat, M., 2017. Grain Size Analysis of Surface Fluvial Sediments in Rivers in Kelantan, Malaysia. Sains Malays. 46, 685–693. https://doi.org/10.17576/jsm-2017-4605-02

Zhang, Y., Song, J., Cheng, D., Zhang, Hangzhen, Zhang, C., Zhang, Haoying, Tang, B., 2025. Effect of sediment particle size distribution characteristics on hyporheic exchange under different riverbed topography. J. Hydrol. 653, 132752. https://doi.org/10.1016/j.jhydrol.2025.13275